



ORIGINAL ARTICLE

Comparative study on the inhibitive effect of Sulfadoxine–Pyrimethamine and an industrial inhibitor on the corrosion of pipeline steel in petroleum pipeline water



N.C. Ngobiri ^{a,c,*}, E.E. Oguzie ^b, N.C. Oforika ^a, O. Akaranta ^a

^a Department of Pure and Industrial Chemistry, University of Port Harcourt (UNIPORT), Nigeria

^b Electrochemistry and Material Research Laboratory, Department of Chemistry, Federal University of Technology, Owerri (FUTO), Nigeria

^c Shell Petroleum Development Company of Nigeria (SPDC), Nigeria

Received 10 February 2014; accepted 8 April 2015

Available online 22 April 2015

KEYWORDS

Adsorption;
Anaerobic;
Corrosion;
Inhibitor;
Modified gravimetric;
Pipeline steel

Abstract The corrosion inhibition characteristics of Sulfadoxine plus Pyrimethamine (S&P) was evaluated and compared with the inhibition performance of an industrial corrosion inhibitor (S-Ind) under anaerobic condition. Modified gravimetric and electrochemical techniques were used. The corrosion inhibition efficiencies of both S&P and S-Ind were comparable for all the techniques applied. S&P gave slightly higher inhibition efficiency, while S-Ind gave a more steady corrosion protection. The corrosion inhibition efficiencies increased with increased concentration of both substances. The polarization curves showed mixed inhibition behavior for both S&P and S-Ind. A mechanism of chemisorption was proposed for the adsorption of S&P and S-Ind on pipeline steel surface, while the negative Gibbs free energy of adsorption values indicates a spontaneous adsorption process. The adsorption characteristics of the inhibitors were fitted into Langmuir adsorption isotherm.

© 2015 The Authors. Production and hosting by Elsevier B.V. on behalf of King Saud University. This is an open access article under the CC BY-NC-ND license (<http://creativecommons.org/licenses/by-nc-nd/4.0/>).

1. Introduction

The use of steel pipes as means of transporting industrial and domestic fluids – crude petroleum, sewage respectively, has been an age long practice. The problem of internal corrosion of these pipes is equally a big industrial and scientific challenge. The internal walls of pipelines are divided into 12, 3, 6 and 9 O' clock positions; the 6 O' clock position in crude oil pipes is more susceptible to internal corrosion because of the

* Corresponding author. Tel.: +234 8037792922.

E-mail address: nnaemekangobiri@yahoo.com (N.C. Ngobiri).

Peer review under responsibility of King Saud University.



Production and hosting by Elsevier

presence of produced water which is denser than oil, low in Oxygen content, with the presence of a variety of microorganisms. The presence of corrosives such as Cl^- , SO_4^{2-} , CO_2 , H_2S , and sulfur reducing bacteria (SRB), contributes to internal corrosion of pipes (Khalifa et al., 2003; Abbasov et al., 2012; Sanni et al., 2013). The interplay of these factors including crude oil composition and chemicals used in oil abstraction makes the crude petroleum pipes prone to worsening pitting corrosion.

An estimate of losses to corrosion indicates that the cost of corrosion is enormous. The effect of pipeline corrosion leakages with the resultant causalities, ecological impact, contamination and shutdowns are some of the consequences of corrosion leakage. The estimated cost corrosion in the United Kingdom and the United States was put at £13.65 billion in 1969 and \$170 billion in 1992 respectively. The adverse effects of corrosion can be reduced drastically by understanding the mechanism and subsequent application of corrosion control measures: injection of chemical inhibitors, electrical-protection, pigging operations and integrity assessment. The use of chemical inhibitors such as rare earth salts, plant extract and synthetic compounds is convenient and cheap (Durnie et al., 1999; Arenas et al., 2001; Aghzzaf et al., 2014).

Organic corrosion inhibitors have been widely applied in solving corrosion problems because of their availability and ease of application. Organic corrosion inhibitors are usually composed of hetero-atoms such as Nitrogen, Sulfur and Oxygen in conjugate systems. The heteroatom is used for adsorption on the surface of the metal (Oguzie, 2007; Obot et al., 2008.). Research results have shown that compounds containing the following functional groups, $-\text{NH}_2$, $-\text{N}=\text{N}$, $\text{C}=\text{N}$, $-\text{S}-\text{CH}_3$, $\text{C}=\text{S}$, $\text{N}-\text{H}$, $-\text{CO}$, $-\text{CNS}$, CHO inhibit the corrosion of metals (Rudesh and Mayanna, 1977; Xueyuan et al., 2001; Morad and El-Dean, 2006; Raymond et al., 2013). These chemical inhibitors are either chemisorbed or physisorbed on the metal surface. The structure–activity relationship and the adsorption data for certain oil field corrosion inhibitors have been used to calculate the kinetics-thermodynamic parameters ($\Delta_{\text{ad}}\text{H}$, $\Delta_{\text{ad}}\text{G}$, $\Delta_{\text{ad}}\text{S}$) and predict their mode of adsorption. Literature shows that compounds that are chemisorbed onto the electrode can yield very good film persistency (i.e. corrosion protection long after injection and at low inhibitor concentration (Durnie et al., 1999)). A lot of research has been carried out on corrosion inhibition with interesting findings which has led to better understanding of corrosion and its inhibition (Kern and Landolt, 2001; Khalifa et al., 2003; Cano et al., 2003). However, most of the inhibitors currently in use in industry poison the environment.

There is search for less negative impact corrosion inhibitors which can compete favorable with existing industrial inhibitors. The corrosion of iron may proceed, depending on the pre-history of the metal and environmental conditions, via different reaction routes. Thus multi-constituent substances, in some instances are required for effective corrosion inhibition synergistic effect (Oguzie, 2004). In the internal walls of pipelines, the combined effect of corrosive elements and microbial consortia necessitates an inhibitor with both anti-oxidative and antimicrobial potentials (Oguzie, 2007; Ngobiri et al., 2013). Corrosion inhibition efficiency can be described as a function of inhibitor's ability to be adsorbed on the metal

surface which is a function of physio-chemical parameters of the inhibitor and the corrosive environment (Ashassi-Sorkhabi and Seifzadeh, 2006; Orubite and Oforka, 2004).

The corrosion inhibition capacity of the combination of Sulfadoxine and Pyrimethamine (S&P) was investigated and compared with an inhibitor currently in use in the petroleum industry named S-Industrial Inhibitor (S-Ind). The presence of sulfur, nitrogen, chlorine and aromatic ring structure in Sulfadoxine + Pyrimethamine (S&P) structure will likely confer a multifunctional advantage on it that is both anti-corrosion and anti-microbial activities. These substance (S&P) have been used as medication against malaria an oxidative stress disease in the ratio of 20:1. The beneficial application of this substance can be increased by investigating its corrosion inhibition potential. Both compounds have the essential heteroatoms for adsorption to the metal surface and aromatic structure with pi electrons (Fig. 1) to stabilize its complex with a metal. The two compounds are unique in their chemical characteristics. Sulfadoxine has a systemic (IUPAC) name, 4-amino-N-(5,6-dimethyl-4-pyridinyl) benzenesulfonamide, a molecular formula of $\text{C}_{12}\text{H}_{14}\text{N}_4\text{O}_4\text{S}$ with a molecular mass of 310 g/mol. While Pyrimethamine has a systemic-IUPAC name: 5-(4-chlorophenyl)-6-ethyl-2,4-pyrimidinediamine, a molecular formula of $\text{C}_{12}\text{H}_{13}\text{ClN}_4$ and molecular weight of 248.71 g/mol.

Corrosion problems have been studied by applying different techniques which including gas-metric, gravimetric, thermometric, surface properties and electrochemistry techniques. Researchers have applied these techniques in understanding the mechanism of corrosion and its inhibition for both natural and synthetic inhibitors. Gravimetric technique has been used to compare the corrosion inhibition properties of *Nypa fruticans* wurmb extract and 1,5-diphenyl-carbazone (Orubite and Oforka, 2004). However, there is a need to stimulate real corrosion environment, hence this work modified the gravimetric method to resemble the internal pipeline environment using Aluminum foil. The temperature inside the pipeline usually does not exceed the day time temperature as most of the oil and gas pipelines are either buried underground or passing through water bodies, which favors the activities of in situ-microorganisms. Also, the electrochemical method was applied to validate the results obtained from the modified gravimetric method.

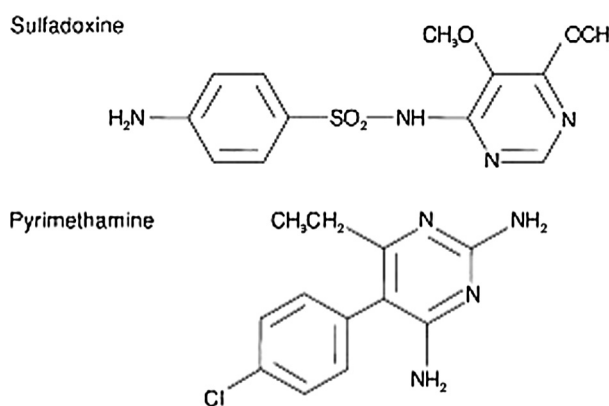


Figure 1 Chemical structure of the inhibitors: Sulfadoxine and Pyrimethamine respectively.

2. Experimental

2.1. Material preparation

Metal sheets from crude oil pipeline steel were obtained from Shell Petroleum Development Company (SPDC) Nigeria's, Pipeline Department and have the chemical composition shown in Table 1. The steel sheets were mechanically pressed into coupons of dimensions of 3 cm × 2.5 cm × 1 cm for the gravimetric experiments. The coupons were perforated with a hole at same position to allow hanging with a polymeric thread. While the working electrode (WE) for the electrochemical experiments was same pipeline steel cut into a quad geometric area of 1 cm², soldered at the rear side to copper wire and imbedded into polytetrafluoroethylene (PTFE) polymer. The steel coupons for both experiments were polished successively with coarse and fine emery paper (from 150 to 2000 grit), decreased in absolute ethanol and dried in acetone.

The electrolyte used was crude oil pipeline water collected with sterile apparatus from the SPDC's Trans Niger Pipeline at Kolo Creek, Balyesa State, Nigeria. The water was stored in a cold chest at 4 °C, and was normalized with experimental environment before use. The test electrolyte was characterized using ASTM standards and previously reported by Ngobiri et al., 2013). All reagents used were of analytical grade and were used without further purification.

2.2. Modified gravimetric experiments

The test corrosion cells were set up by suspending (with polymeric thread) the pre-cleaned and weighed steel coupons inside five different 250 ml Glass beakers filled with 200 ml crude oil pipeline water (total immersion or weight loss test), containing diluents range of 10⁻²–10⁻⁵ M for each of the additive at 28 ± 1 °C. The fifth coupon was set up without any additive. Okafor et al., 2008, Karthikaiselvi et al., 2012 have previously used similar method. However, Aluminum foil of 25 μm known for its impermeability to air, light and water, was used to tight seal the entire test corrosion cells in order to stimulate an anaerobic environment. This procedure has been previously reported by Ngobiri et al., 2013. The pipeline coupons were retrieved at 7 day (168 h) intervals. The coupons were washed several times with the aid of a brittle brush inside water to remove corrosion products, degreased with ethanol, dried in acetone and allowed to air dry to a constant weight. The experiment was performed in triplicate to ensure reproducibility. The average weight of the three coupons was used as the weight of a corrosion cell coupon. The experiment was allowed to run for five weeks. The weight loss was calculated in grams as the difference between the initial weight before immersion and the constant weight after the removal of corrosion products.

Table 1 Chemical composition of pipeline steel.

Element	C	S	P	Si	Mn	Al	Fe
Composition (wt.%)	0.47	0.005	0.003	0.24	1.44	0.01	Balance

2.3. Electrochemical measurements

The electrochemical experiments were carried out using the conventional three-electrode cell with a platinum counter electrode, a saturated calomel electrode (SCE) coupled to a fine Luggin capillary as reference electrode. The cell was covered in a manner similar to the gravimetric cell. All the experiments were carried out at open circuit potential (OCP) for 30 min to attain a stable potential. The experiments were all carried out using a Perstat 2273 Advanced Electrochemical system. Each experiment was repeated three times to ensure reproducibility.

The potentiodynamic polarization (PDP) experiments were started at the cathodic potential of -250 mV to anodic potential of +250 mV at a scan rate of 1 mV s⁻¹. Corrosion current density (I_{corr}), equilibrium corrosion potential (E_{corr}) and other Tafel parameters were extrapolated using the power suite software. Corrosion inhibition efficiency (η_p (%)) was defined as follows:

$$\eta_p (\%) = \frac{I_{\text{corr}}^0 - I_{\text{corr}}^i}{I_{\text{corr}}^0} \times 100 \quad (1)$$

where I_{corr}^0 and I_{corr}^i are corrosion current densities in the uninhibited and inhibited systems respectively.

Electrochemical impedance spectroscopy (EIS) experiments were carried out between frequencies of 100 kHz to 10 mHz using a signal of 10 mV amplitude. Electrochemical impedance data were derived using ZsimpWin software. The corrosion inhibition efficiency η_E (%) was determined by applying the charge transfer resistance (R_{ct}) with the relationship:

$$\eta_E (\%) = \frac{R_{\text{cti}} - R_{\text{ct}}}{R_{\text{cti}}} \times 100 \quad (2)$$

where R_{cti} and R_{ct} are the charge transfer resistance in the presence and absence of the additives respectively.

2.4. Surface morphology observation

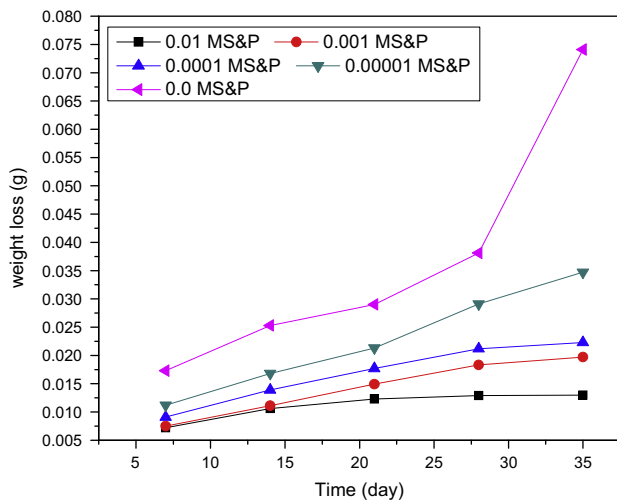
The surface morphology characterization was carried out using Oxford x-Max Scanning Electron Microscope (SEM). The test pipeline steel coupons were prepared as described for the electrochemical experiment above. One was immersed in crude oil pipeline water while the second and third coupons were immersed in solutions of crude oil pipeline water with 0.01 M S&P and S-Ind respectively for 24 h. The coupons were retrieved, rinsed, dried and subjected to SEM examination.

3. Results and discussion

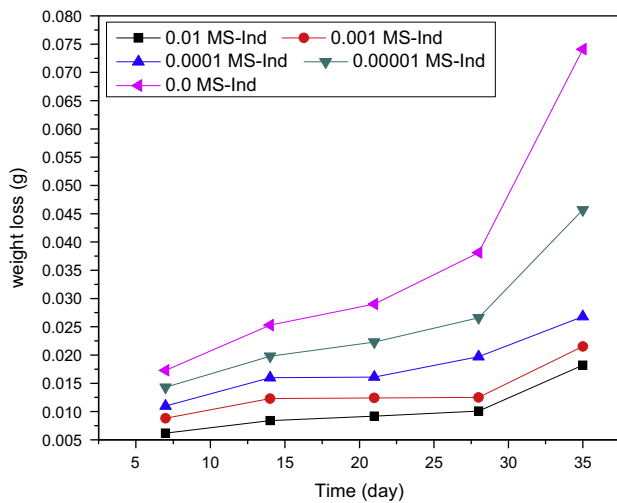
3.1. Modified gravimetric results

3.1.1. Weight loss and corrosion rate

The corrosion behavior of pipeline steel in produced water with limited oxygen content was monitored using a modified gravimetric technique. The weight loss and corrosion rate as indicators of corrosion trend were plotted in Figs. 2 and 3. Fig. 2 presents the rate of loss of iron in petroleum pipeline water in the presence and absence of (a) S&P and (b) S-Ind. The results indicate that metal dissolution in produced water environment increased with time and decreased with increase in concentration of the additives, confirming that both the



(a)



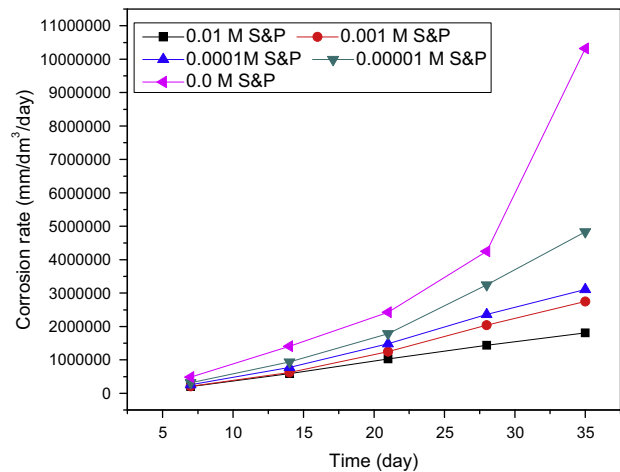
(b)

Figure 2 Variation of weight loss with time for pipeline steel in produced water with different concentrations of (a) S&P and (b) S-Ind.

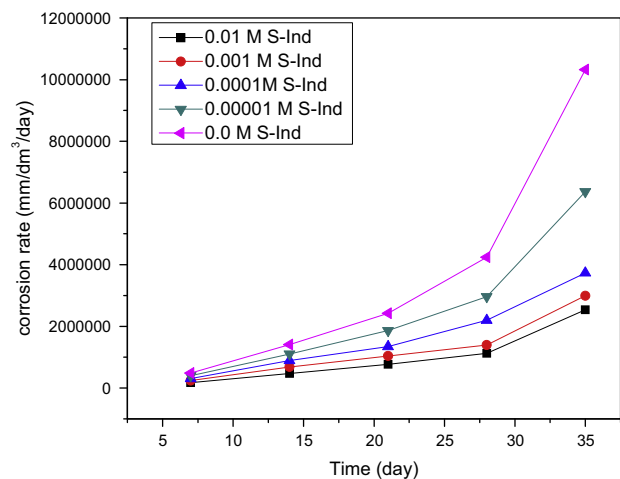
additives, S-Ind and S&P were able to reduce the rate of metal dissolution. It is believed that organic corrosion inhibitors inhibit corrosion by getting adsorbed on the metal surface, thereby separating the metal from the corrodant (Ebenso et al., 2002; Ekpe et al., 1995) or blocking the corrosion active sites (Okafor and Zheng, 2009). The non-uniformity of the plots indicates that corrosion is not a simple homogenous process but a heterogeneous process (Orubite and Oforka, 2004). It then follows, that corrosion control can be achieved with different techniques with varying results including use of chemical inhibitors.

The corrosion rate of pipeline steel in petroleum pipeline water, and in the presence and absence of different concentrations of the project additives was evaluated from weight loss data using

$$CR_{(\text{Mg}/\text{dm}^2/\text{day})} = \frac{\Delta w(\text{mg}) \times 10^3}{\text{Area}/100 \times \text{day}} \quad (3)$$



(a)

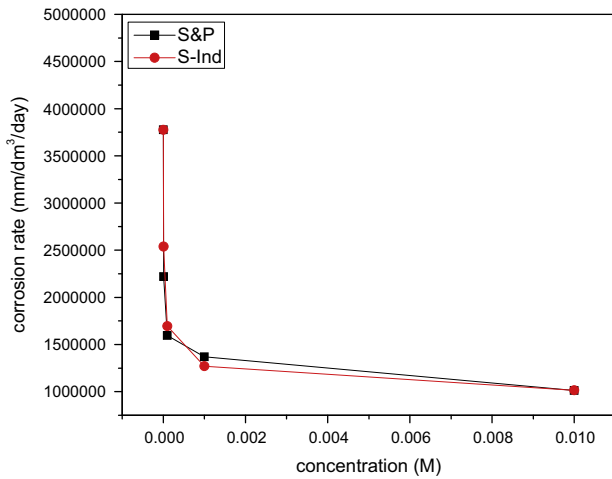


(b)

Figure 3 Variation of corrosion rate with time for pipeline steel in produced water with different concentrations of (a) S&P and (b) S-Ind.

where CR is corrosion rate and Δw is the change in coupon weight (Hasan and Sisodia, 2011).

The results obtained were plotted as a function of time and shown in Fig. 3. Fig. 3 shows the corrosion rate trend for (a) S&P and (b) S-Ind in petroleum pipeline water. The results of the blank experiment showed an aggressive attack on pipeline steel under the test environment. The addition of both S&P and S-Ind reduced the corrosion rate at all concentrations tested. The most significant reduction was recorded at 0.01 M for both additives which is in agreement with the trend of other research finding (Chauhan and Gunasekaran, 2007; Jeyaprabha., 2006; Tang et al., 2006; Oguzie et al., 2004). Assuming inhibitors function by adsorption at the metal surface the corrosion rate can be related to inhibitor concentration and surface coverage. The corrosion rates increased with time at all additive concentrations tested. S-Ind, showed a sharp rise in corrosion rate at all experimental concentrations after four weeks suggesting that it has high desorption potential at the metal surface after four weeks (Tang et al., 2006).



(c)

Figure 3c Variation of the average Corrosion rate of pipeline steel in produced water with different concentrations of S&P and S-Ind.

The 0.01 M S&P did not show this character throughout the experimental duration. The 0.01 M S&P is suitable for more prolonged application, while the application of S-Ind should not exceed monthly application.

Fig. 3c, illustrates the corrosion rate of S&P and S-Ind as function of concentration. From Fig. 3c, it is shown that S&P and S-Ind exhibited comparable corrosion rates at all experimental concentrations. However, from the plot as the concentration of both inhibitors approach 10^{-4} M, the corrosion rate raised linearly. The corrosion rate varied indirectly with concentration and surface coverage. Consequently, the reduction in corrosion rate by S&P and S-Ind can be associated with the number of corrosion active sites the additives was able to block on the metal surface through adsorption, consequently the unblocked sites determine the corrosion rate (Oguzie et al., 2004).

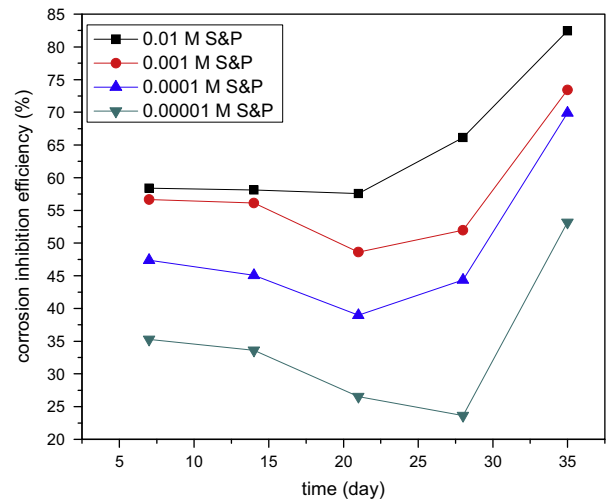
3.1.2. Surface coverage and inhibition efficiency

Assuming, that corrosion on the metal surface occurs in the inhibitor unblocked sites, such that covered site has zero corrosion rate. The degree of surface coverage (θ) of S&P and S-Ind on pipeline steel in petroleum pipeline water was calculated using Eq. (4).

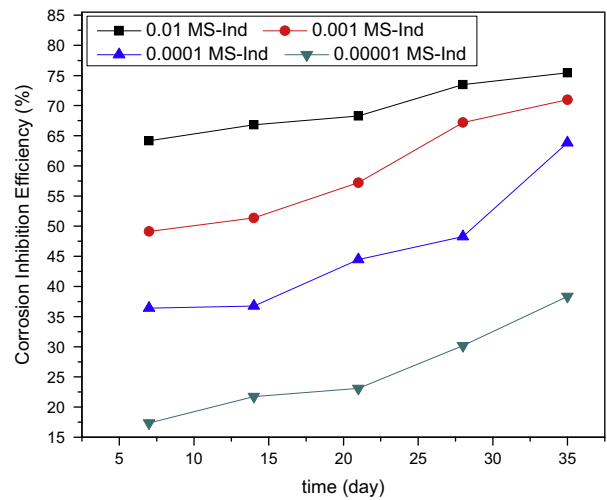
$$\theta = 1 - \frac{CR_{inh}}{CR_{blank}} \tag{4}$$

where CR_{inh} and CR_{blank} are the corrosion rates in the absence and presence of S&P and S-Ind (Oguzie et al., 2004). The surface coverage increased with increase in S&P and S-Ind concentration and generally decreased with time for both additives. The ability of S&P and S-Ind to cover the surface of pipeline steel surface reduced the corrosion rate, thereby improving the inhibition efficiency of the additives.

$$\eta = \left(1 - \frac{CR_{inh}}{CR_{blank}}\right) \times 100 \tag{5}$$



(a)



(b)

Figure 4 Variation of corrosion inhibition efficiency with time of (a) S&P and (b) S-Ind for corrosion pipeline steel in petroleum pipeline water.

The corrosion inhibition efficiency of S&P and S-Ind was calculated from the corrosion data using Eq. (5). The results obtained were plotted versus time and presented in Fig. 4(a) S&P and (b) S-Ind. From Fig. 4, the inhibition efficiencies of both S&P and S-Ind increased significantly with increased concentration of both additives (Kavipriya et al., 2013). The highest inhibition efficiency exhibited by S&P was 78.85%, while S-Ind was 75.44% at 0.01 M inhibitor concentration. S&P displayed slightly higher inhibition efficiency, while S-Ind tends to offer steady corrosion protection to the metal compared with the S&P which showed lower efficiency for approximately three weeks and raised the inhibition efficiency afterward. The results obtained further confirm the comparability of corrosion inhibition efficiency of both S&P and S-Ind. The variation of average corrosion inhibition efficiency of S&P and S-Ind with concentration was plotted and presented in Fig. 4c. S-Ind exhibited higher corrosion inhibition efficiencies than S&P at higher concentrations.

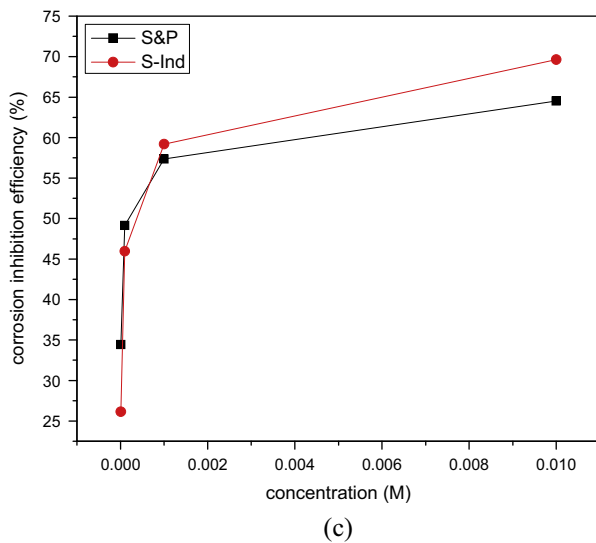


Figure 4c Comparison of corrosion inhibition efficiency of S&P and S-Ind with concentration for pipeline steel in pipeline water.

3.1.3. Kinetics and mechanism of corrosion inhibition of S&P and S-Ind for pipeline steel in pipeline water

The logarithm of the initial weight of pipeline steel minus the weight loss of pipeline steel in petroleum pipeline water $\log(w - \Delta w)$, in the presence and absence of S&P and S-Ind was plotted against time and presented in Fig. 5, Fig. 5a and b respectively shows the kinetics of the corrosion process for S&P and S-Ind respectively. Fig. 5, reveals a linear plot for all the data plotted indicating that the corrosion of pipeline steel in the pipeline water is of first order kinetics.

The corrosion rate constant K , and material half life $t_{1/2}$ were also calculated from the weight loss data for first order reaction using Eqs. (6) and (7) respectively,

$$K = \frac{2.303}{\text{Time}} \log \frac{w_i}{w_f} \quad (6)$$

where w_i and w_f are the initial and final weight of the metal coupons respectively.

$$t_{1/2} = \frac{0.693}{k} \quad (7)$$

The results obtained at various concentrations were averaged and presented in Table 2, while Fig. 6 presents the plot of the variation of material half life for different concentrations of S&P and S-Ind. The additives were both able to increase the half life and reduce the corrosion rate constant, which indicates that both S&P and S-Ind have the ability to increase corrosion activation energy with consequent longer material half life.

The corrosion rate constant K decreased with increase in S&P and S-Ind concentrations, while the material half life increased with increase in the concentrations of both S&P and S-Ind. At concentration of less than 10^{-3} , the rate constant increases sharply while the material half life decreases sharply for both additives. The relationship between corrosion rate constant K and material half life is an inverse relationship (Eqs. (6) and (7)). Though, the corrosion rate constant and material half life $t_{1/2}$ for both S&P and S-Ind are comparable, S&P showed higher average rate constant, while S-Ind showed

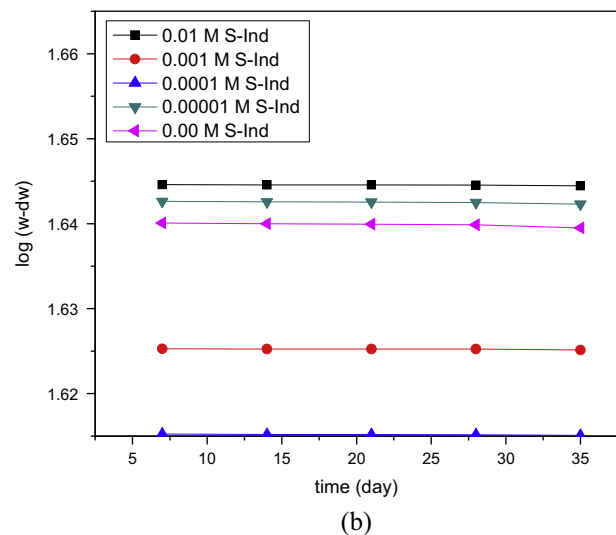
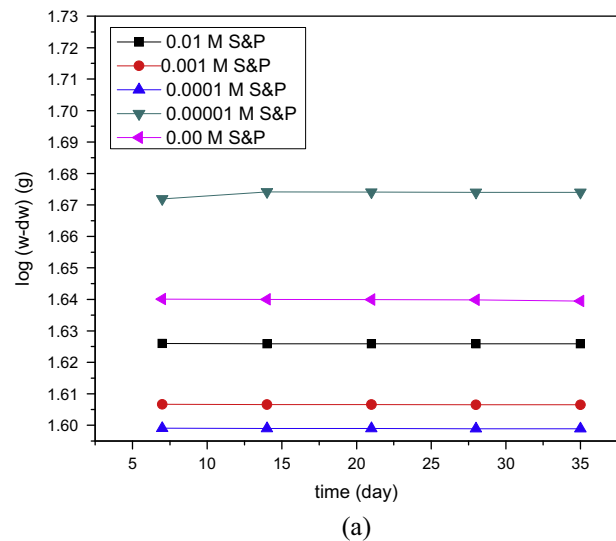


Figure 5 Plot of $\log(w - \Delta w)$ versus time for the corrosion of pipeline steel in pipeline water in the presence and absence of (a) S&P and (b) S-Ind.

Table 2 Variation of corrosion rate constant and half life data for pipeline steel in pipeline water with different concentrations of S&P and S-Ind.

Concentration (M)	S&P		S-Ind	
	Rate constant (k)	$t_{1/2}$ (days)	Rate constant (k)	$t_{1/2}$ (days)
0.00001	4.36×10^{-5}	15903.75	4.19×10^{-5}	16552.38
0.0001	3.36×10^{-5}	21283.37	3.35×10^{-5}	20676.04
0.001	2.80×10^{-5}	24764.24	2.61×10^{-5}	26559.94
0.01	2.40×10^{-5}	28842.11	2.09×10^{-5}	33146.96

longer average material half life at higher concentrations. This is in agreement with the percentage corrosion inhibition efficiency data. Corrosion rate constant K and material half life $t_{1/2}$ are therefore can be useful parameters in material integrity assessment.

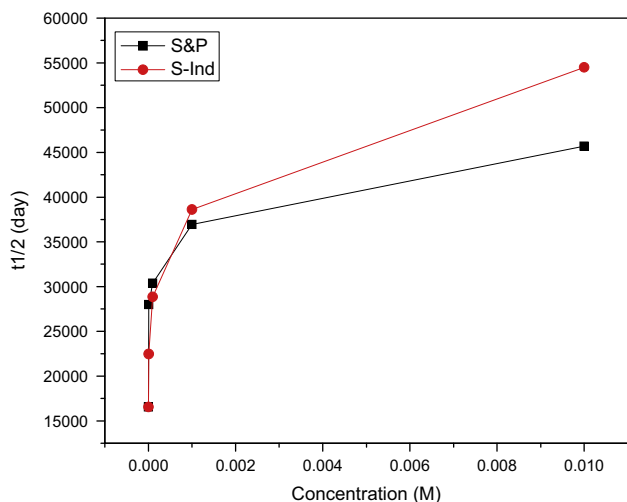


Figure 6 Variation of material half life for different concentrations of S&P and S-Ind inhibitors.

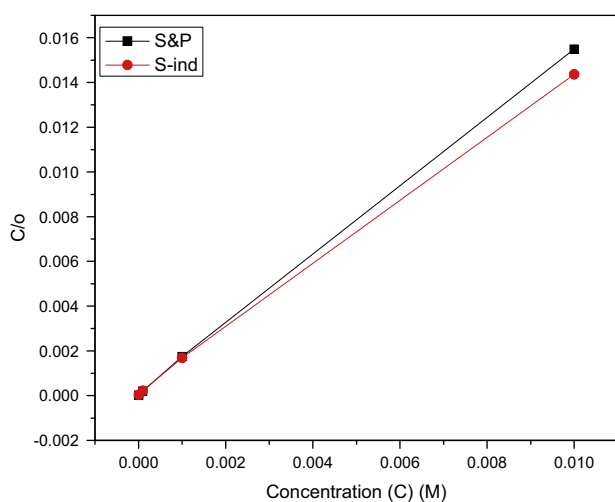


Figure 7 Langmuir adsorption isotherm for the adsorption of S&P and S-Ind on pipeline steel in pipeline water.

3.1.4. Adsorption consideration

The understanding of the mechanism of corrosion inhibition by organic corrosion inhibitors is predicated on the understanding of the adsorption behavior of inhibitor molecules on the metal surface. This is dependent on the charge/electron density of the inhibitor molecule, the nature and charge of the metal surface and the bio-chemical characteristics of the corroding environment, which also determines the extent of surface coverage of the inhibitor on the electrode. Adsorption proceeds through two different modes. The first is physical adsorption which requires the presence of charged surface entities and opposite charged chemical entities in the bulk solution to achieve weak chemical interaction. The second is chemisorption which proceeds through charge transfer and charge sharing between the inhibitor and the metal surface, resulting to a strong chemical interaction (Ebenso et al., 2002). Usually, there is a vacant lower energy d electron orbital in iron, while the inhibitor possesses free electrons or lone-pair

Table 3 Calculated values of Gibbs free energy of adsorption and surface coverage for corrosion inhibition of pipeline steel by S&P and S-Ind in pipeline water.

Conc. (mol/dm ³)	ΔG_{ad} (S&P) (kJ/mol)	ΔG_{ad} (S-Ind) (kJ/mol)	θ (S&P)	θ (S-Ind)
0.00001	-33.76	-32.43	0.34	0.26
0.0001	-30.65	-29.76	0.49	0.50
0.001	-26.21	-26.55	0.57	0.59
0.01	-22.21	-23.08	0.65	0.70

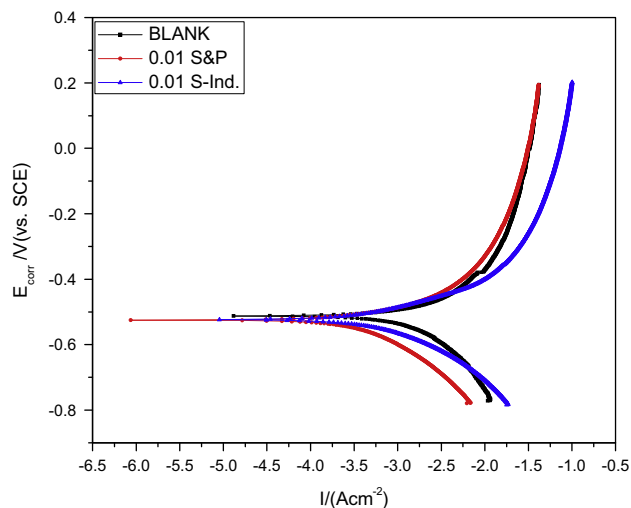


Figure 8 Potentiodynamic polarization curve for pipeline steel in petroleum pipeline water in the presence and absence of S&P and S-Ind.

Table 4 Potentiodynamic polarization parameters for pipeline steel in petroleum pipeline water in the presence and absence of S&P and S-Ind.

Additive Conc.	Blank	0.01 M S&P	0.1 M S-Ind
Eff (%)		77.64	74.07
I_{corr} (A/cm ²)	6.44×10^{-3}	1.44×10^{-3}	1.67×10^{-3}
β_c (mV dec ⁻¹)	808.32	333.11	213.62
B_a (mV dec ⁻¹)	625.22	219.10	168.54
E_{corr} (mV versus SCE)	-542.98	-538.84	-529.74

electrons which is usually available to fill the vacant metallic orbital.

Fig. 7 and Table 3 indicate that the corrosion inhibition efficiency of S&P and S-Ind is dependent on their concentration (C) and consequent surface coverage (θ). The adsorption behavior of these substances on the metal surface was determined graphically by plotting the surface coverage and concentration data to determine the best fitted adsorption isotherm. The linear plot of C/θ against C confirms that the project inhibitors adsorb according to Langmuir's isotherm. Research has reported the adsorption of inhibitor molecules to be a

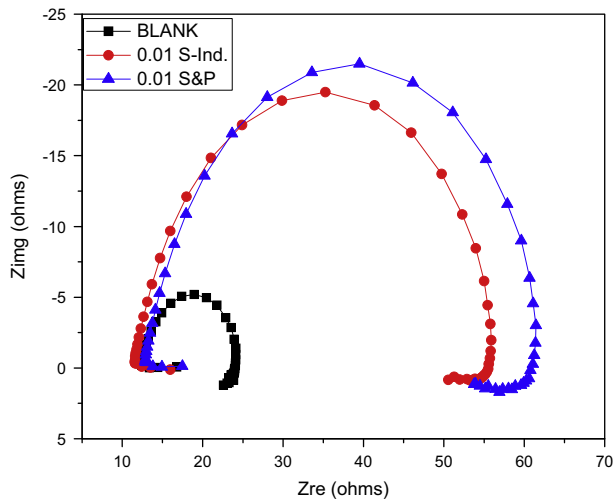


Figure 9 Nyquist plot for pipeline steel in petroleum pipeline water with and without S&P and S-Ind.

quasistatistical process, was water molecules first get adsorbed on the electrode surface. The organic inhibitor molecules get adsorbed on the metal/solution interface through the substitution of the already adsorbed water molecule (Bockris and Swinkels, 1964). The difference in molecular size and chemical properties has the tendency to affect substitution rate. These may account for the time taken to attain the highest inhibition efficiency which was faster with S&P. Also, the non 100% corrosion inhibition efficiency and surface coverage

of 1 explain the persistence of corrosion even in the presence of S&P and S-Ind (Ngobiri et al., 2015).

The nature of interaction between the metal surface with S&P and S-Ind was obtained using free energy of adsorption, ΔG_{ads} was calculated using the relationship:

$$\Delta G_{\text{ads}} = -2.303RT \log \left[\frac{55.4\theta}{C_0(1-\theta)^n} \frac{\{\theta + (1-\theta)n\}^{n-1}}{n^n} \right] \quad (8)$$

where C_0 is the concentration of inhibitor in the bulk of the solution; n is the size factor (9 for flat adsorption on the surface and 3 in the perpendicular direction to the surface), θ is the surface coverage, T represents the absolute temperature and R is the thermodynamic gas constant.

From Table 3, the negative values of ΔG_{ads} show that the adsorption of S&P and S-Ind was a spontaneous process and was strong on the steel surface. However, the not so high negative values are suggestive of chemical adsorption at lower concentrations (Atkins and Paula, 2002).

3.2. Electrochemical studies

3.2.1. Potentiodynamic polarization studies

The potentiodynamic polarization curve of pipeline steel in petroleum pipeline water under pseudo-anaerobic condition with and without various concentrations of S&P and S-Ind are presented in Fig. 8. The Tafel parameters—equilibrium corrosion potential (E_{corr}), corrosion current density (I_{corr}), cathodic Tafel slope (β_c), anodic Tafel slope (β_a) and corrosion inhibition efficiency associated with Fig. 8 are presented in Table 4. Table 4, indicates a reduction in the cathodic Tafel

Table 5 Impedance parameters for pipeline steel in petroleum pipeline water with and without S&P and S-Ind.

Additives	Conc. (M)	R_s ($\Omega \text{ cm}^2$)	R_{ct} ($\Omega \text{ cm}^2$)	R_{ind} ($\Omega \text{ cm}^2$)	CPE (S-sec ⁿ /CM ²)	n	L (H cm ²)	η (%)
BLANK	—	13.40	10.86	41.51	0.00012	0.8	615.0	—
S&P	0.01	13.58	48.02	319.80	7.79E-5	0.9184	323.6	77.4
S-Ind	0.01	12.23	43.81	474.80	8.74E-5	0.9199	752.1	75.2

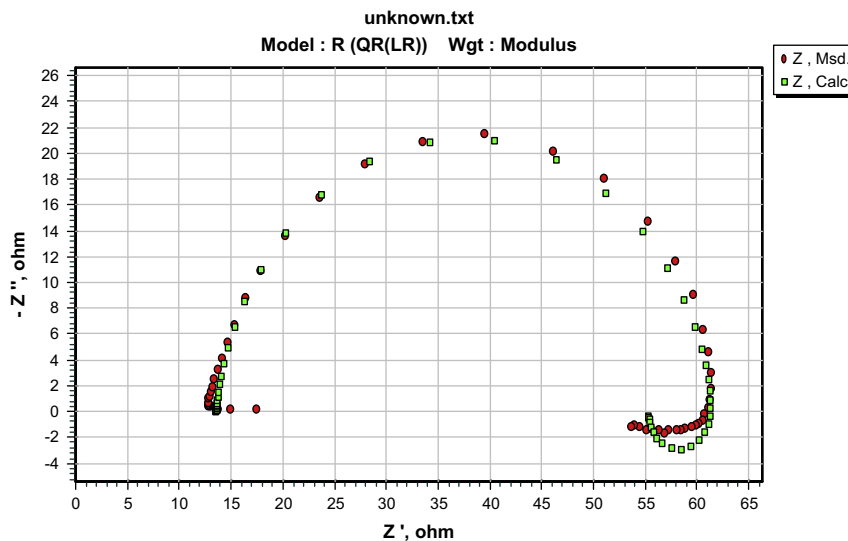


Figure 10 ZsimpWin plot of experimental and computer impedance data for pipeline steel in petroleum pipeline water with 0.01 S&P.

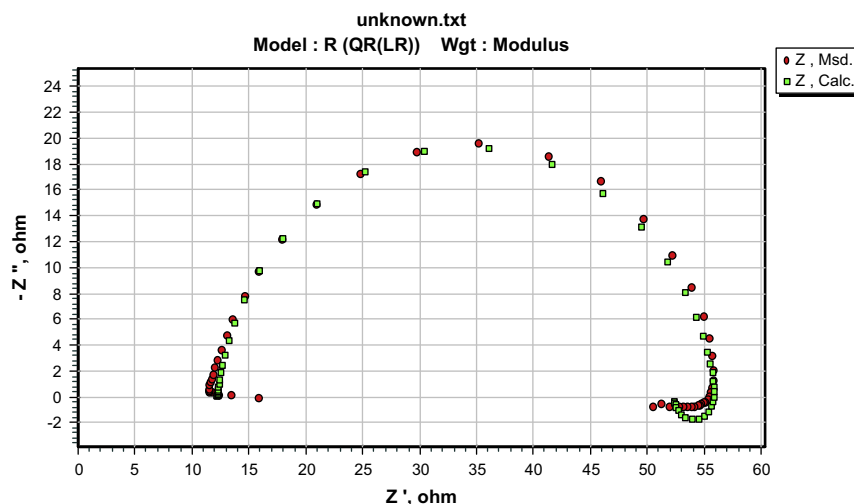


Figure 11 ZsimpWin plot of experimental and computer impedance data for pipeline steel in petroleum pipeline water with 0.01 S-Ind.

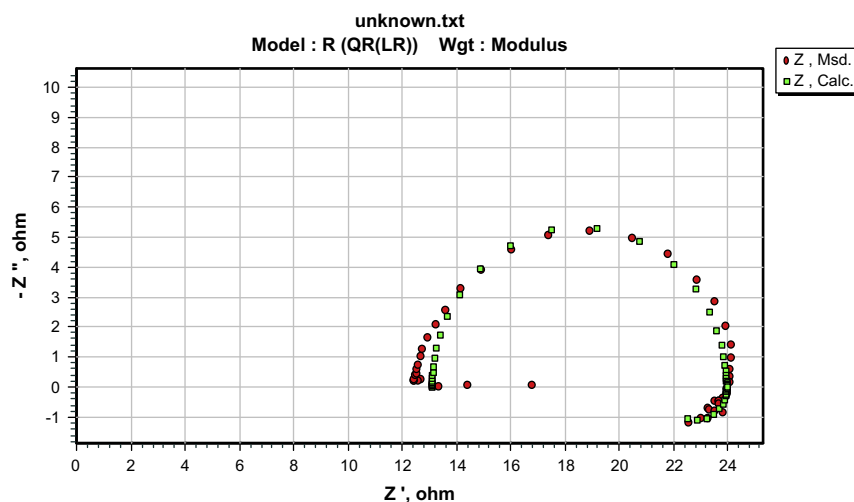


Figure 12 ZsimpWin plot of experimental and computer impedance data for pipeline steel in petroleum pipeline water.

slope, anodic Tafel slope and corrosion current density and an increase in equilibrium corrosion potential due to the presence of S&P and S-Ind. This is an indication of corrosion inhibition ability of S&P and S-Ind. S&P and S-Ind can be classified as mixed type corrosion inhibitor because of the abilities to reduce both the cathodic and anodic currents (Li et al., 2008). The slight variation in corrosion inhibition efficiency between potentiodynamic polarization and modified gravimetric can be attributed to varying degree of sealing off oxygen from the corrosion cells due to the manual nature of the sealing.

3.2.2. Electrochemical impedance spectroscopy

Electrochemical impedance spectroscopy has been used previously to acquire information on the corrosion inhibition mechanism at the metal-electrolyte interface, because it provides information on the resistive and capacitive behavior at the interface (Li et al., 2008; Ashassi-Sorkhabi and Seifzadeh, 2006). The electrochemical impedance spectra were measured at corresponding open circuit potential. The electrochemical

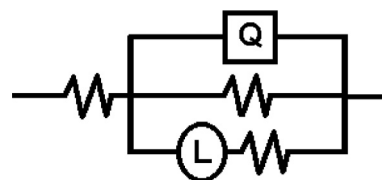


Figure 13 Electrochemical equivalent circuit for impedance response of pipeline steel in petroleum pipeline water with and without S&P and S-Ind.

impedance Nyquist plot for pipeline steel in petroleum pipeline water with and without S&P and S-Ind is depicted in Fig. 9. The impedance spectra for pipeline steel in petroleum pipeline water with and without the project additives are characterized by a high frequency capacitive loop and a low frequency inductive loop. The semicircular shaped plots with center under the x-axis for the three experiments indicate the corrosion process is mainly controlled by the charge transfer process. Also, the

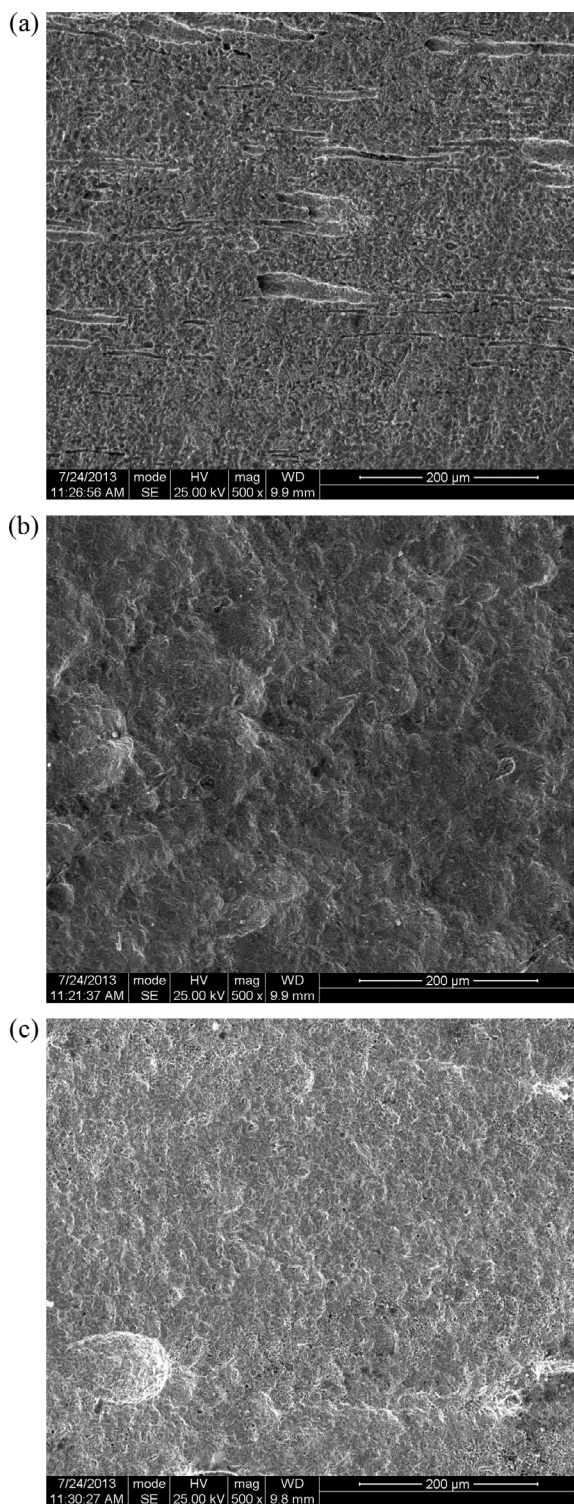


Figure 14 SEM images of pipeline steel in petroleum pipeline water (a) without S&P and S-Ind, (b) with S&P, and (c) with S-Ind.

semicircles are characteristic of solid electrodes. The increase in the diameter of the capacitive loops in the presence of S&P and S-Ind is an indication of the corrosion inhibition behavior of the additives. The low frequency inductive loop has been previously attributed relaxation process due to

adsorption of species like Cl_{ads}^- and H_{ads}^+ on the electrode surface (Amin et al., 2007) and redissolution of passivated surface at low frequency (Sherif et al., 2006).

The similarity in the shapes of the impedance spectra in the presence and absence of the additives indicates that both S&P and S-Ind do not change the corrosion mechanism (Ngobiri et al., 2015). The impedance spectra in Fig. 9 were analyzed using ZsimpWin software by applying the equivalent circuit model $R(QR(LR))$ in Fig. 13. The impedance parameters are presented in Table 5 while the ZsimpWin plot of experimental and computer impedance data for pipeline steel in petroleum pipeline water with S&P, S-Ind and without the additive is presented in Figs. 10–12 respectively. Figs. 10–12 show that the experimental data are fitted to the model. The results obtained from the electrochemical impedance spectra were close to the modified gravimetric and polarization methods. The slight variation maybe attributed minor degree of experimental error.

3.3. Corrosion surface morphology

Fig. 14 presents scanning electron microscope (SEM) images of Pipeline steel in petroleum pipeline water (a) without S&P and S-Ind, (b) with S&P, (c) with S-Ind respectively. The corrosion surface of Fig. 14(a) is rougher while Fig. 14(b) and (c) was smoother confirming the corrosion retarding properties of S&P and S-Ind. The results of the electrochemical impedance studies indicate that both substances inhibited the corrosion pipeline steel in petroleum pipeline water by getting adsorbed on the pipeline steel surface. However, there is still a level of corrosion damage on the steel surface. Several reasons have been adduced to this by these researchers (Ngobiri et al., 2015).

4. Conclusion

The corrosion of crude oil pipeline steel in pipeline water environment was inhibited by S&P and S-Ind. Both inhibitors showed comparable inhibition efficiencies with the three techniques applied. The mechanism of inhibition was attributed to adsorption of the inhibitors on the steel surface. The process was approximated to Langmuir adsorption isotherm while the values of their Gibbs free energy of adsorption show that the adsorption of both inhibitors strong and spontaneous.

Acknowledgments

N.C.N. acknowledges Tertiary Education Trust Fund, (tetfund, Nigeria Grant – TETFUND/ES/AST&D/UNIV/PH/VOL.1), Shell Petroleum Development Company of Nigeria (SPDC-2010/11 INTERN), and Metal Research Institute – State Key Laboratory for Corrosion and Protection, Shenyang China. Also, L.C. Chiejina and S. D. Jackreese are acknowledged for efforts in providing the industrial inhibitor and facilitating SPDC laboratory space.

References

- Abbasov, V.M., Ezizbeyli, A.R., Jafarova, R.A., Hajiyeva, S.Y., Gasimov, E.E., 2012. Corrosion inhibition of steel C 1018 with novel complex of imidazoline. *Chem. J.* 2 (06), 194–198.

- Aghzaf, A.A., Rhouta, B., Rocca, E., Khalil, A., Steinmetz, J., 2014. Corrosion inhibition of zinc by calcium exchanged beidellite clay mineral: a new smart corrosion inhibitor. *Corros. Sci.* 80, 46–52.
- Amin, M.A., Abd El-Rehim, S.S., El-Shebini, E.E.F., Bayyomi, R.S., 2007. The inhibition of low carbon steel corrosion in hydrochloric acid solution by succinic acid – Part 1: Weight loss, polarization, EIS, PZC, EDX, and SEM studies. *Electrochim. Acta* 38, 3588–3600.
- Arenas, M.A., Bethencourt, M., Botana, F.J., De Damborenea, J., Marcos, M., 2001. Inhibition of 5083 aluminium alloy and galvanized steel by lanthanide salts. *Corros. Sci.* 43, 157–170.
- Ashassi-Sorkhabi, H., Seifzadeh, D., 2006. The inhibition of steel corrosion in hydrochloric acid solution by juice of prunus cerasus. *Int. J. Electrochem. Sci.* 1, 92–98.
- Atkins, P., Paula, J., 2002. *Atkins Physical Chemistry*, seventh ed. Oxford University Press, UK, p. 989.
- Bockris, J.O.M., Swinkels, D.A.J., 1964. Adsorption of n-Decylamine on solid metal electrodes. *J. Electrochem. Soc.* 111, 736–743.
- Cano, E., Pinilla, P., Polo, L.J., Bastida, J.M., 2003. Copper corrosion inhibition by fast green, fuchsin acid and basic compounds in citric acid solution. *Mater. Corros.* 54, 222–228.
- Chauhan, L.R., Gunasekaran, G., 2007. Corrosion inhibition of mild steel by plant extracts in dilute HCl medium. *Corros. Sci.* 49, 1147.
- Durnie, W., De Marco, R., Jefferson, A., Kinsella, B., 1999. Structure activity of oil field corrosion inhibitors. *J. Electrochem. Soc.* 146 (5), 1751–1756.
- Ebenso, E.E., Okafor, P.C., Ekpe, U.J., 2002. Studies on the inhibition of aluminium corrosion by 2-acetylphenothiazine in chloroacetic acids. *Bull. Electrochem.* 18 (12), 551–558.
- Ekpe, U.J., Ibok, U.J., Ita, B.I., Ofiong, O.E., Ebenso, E.E., 1995. Inhibitory action of methyl and phenyl thiosemicarbazone derivatives on the corrosion of mild steel in hydrochloric acid. *Mater. Chem. Phys.* 40, 87–93.
- Hasan, S.K., Sisodia, P., 2011. Paniaia (*Flacourtia Jangomas*) plant extract as eco friendly inhibitor on the corrosion of mild steel in acidic media. *Rasayan J. Chem.* 4 (3), 548–553.
- Jeyaprabha, C., Sathiyarayanan, S., Venkatachari, G., 2006. Influence of halide ions on the adsorption of diphenylamine on iron in 0.5 M H₂SO₄ solutions. *Electrochim. Acta* 51, 4080–4088.
- Karthikaiselvi, R., Subhashini, S., Rajalakshmi, R., 2012. Poly(vinyl alcohol–aniline) water soluble composite as corrosion inhibitor for mild steel in 1 M HCl. *Arab. J. Chem.* 5, 517–522.
- Kavipriya, K., Sathiyabama, J., Rajendran, S., Nagalakshmi, R., 2013. The inhibitive effect of diethylene phosphonic acid on the corrosion of carbon steel in sea water. *Eur. Chem. Bull.* 2 (7), 423–429.
- Kern, P., Landolt, D., 2001. Adsorption of organic inhibitor on iron and gold studied with a rotating EQCM. *J. Electrochem. Soc.* 148 (6), B228–B235.
- Khalifa, M.A., El-Batouti, M., Mahgoub, F., Bakr Aknish, A., 2003. Corrosion inhibition of steel in crude oil storage tanks. *Mater. Corros.* 54, 251–258.
- Li, W., He, Q., Zhang, S., Pei, B., Hou, B., 2008. Some new triazole derivatives as inhibitors for mild steel corrosion in acid medium. *J. Appl. Electrochem.* 38 (3), 289–395.
- Morad, M.S., El-Dean, A.M.K., 2006. 2,2'-dithiobis(3-cyno-4,6-dimethylpyridine): a new class of acid corrosion inhibitors for mild steel. *Corros. Sci.* 48, 3398–3412.
- Ngobiri, N.C., Akaranta, O., Oforka, N.C., Oguzie, E.E., Ogbulie, S.U., 2013. Inhibition of pseudo-anaerobic corrosion oil pipeline steel in pipeline water using biomass-derived molecules. *Adv. Mater. Corros.* 2, 20–25.
- Ngobiri, N.C., Oguzie, E.E., Li, Y., Liu, L., Oforka, N.C., Akaranta, O., 2015. Eco-friendly corrosion inhibition of pipeline steel using *Brassica Oleracea*. *Int. J. Corros.* Article ID 404139, 1–9.
- Obot, I.B., Ebenso, E.E., Gasem, Z.M., 2008. Eco-friendly corrosion inhibitor: adsorption and inhibitive action of ethanol extract of *Chlomolaena Odorata* L. for the corrosion of mild steel in H₂SO₄ solution. *Int. J. Electrochem.* 7, 1998.
- Oguzie, E.E., 2004. Influence of halide ions on the inhibitive effect of Congo red dye on the corrosion of mild steel in sulphuric acid solution. *Mater. Chem. Phys.* 87, 212–217.
- Oguzie, E.E., 2007. Corrosion inhibition of aluminium in acidic and alkaline media by *Sansevieria trifasciata* extract. *Corros. Sci.* 49, 1527–1539.
- Oguzie, E.E., Unaegu, C., Ogukwe, C.N., Okolue, B.N., Onuchukwu, A.I., 2004. Inhibition of mild steel corrosion in sulphuric acid using indigo dye and synergistic halide additives. *Mater. Chem. Phys.* 84, 363–368.
- Okafor, P.C., Zheng, Y., 2009. Synergistic inhibition of methylbenzyl quaternary imidazoline derivative and iodide ions on mild steel in H₂SO₄ solutions. *Corros. Sci.* 51, 850–859.
- Okafor, P.C., Ikpi, M.E., Uwah, I.E., Ebenso, E.E., Ekpe, U.J., Umoren, S.A., 2008. Inhibitory action of *Phyllanthus amarus* extracts on the corrosion of mild steel in acidic media. *Corros. Sci.* 50, 2310–2317.
- Orubite, K.O., Oforka, N.C., 2004. Inhibition of the corrosion of mild steel in hydrochloric acid solution by extracts of leaves of *Nypa Fruticans* Wurmb. *Mater. Lett.* 58, 1768–1772.
- Raymond, P.P., Regis, P.P.A., Rajendram, S., Manivannan, M., 2013. Investigation of corrosion inhibition of stainless steel by sodium tungstate. *Res. J. Chem. Sci.* 3 (2), 54–58.
- Rudesh, H.B., Mayanna, S.M., 1977. Adsorption of n-Decylamine on zinc from acidic chloride solution. *J. Electrochem. Soc.* 124 (3), 340–342.
- Sanni, O., Loto, C.A., Popoola, A.P.I., 2013. Effect of ferrous gluconate inhibition on the electrochemical behaviour of mild steel in 3.5% NaCl. *Int. J. Electrochem. Sci.* 8, 5506–5514.
- Sherif, E.M., Park, S.M., 2006. Effect of 1,4-naphthoquinone on aluminum corrosion in 0.5 M sodium chloride solutions. *Electrochim. Acta* 51 (7), 1313–1321.
- Tang, L., Li, X., Mu, G., Liu, G., Li, L., Liu, H., Si, Y., 2006. The synergistic inhibition between hexadecyl trimethyl ammonium bromide (HTAB) and NaBr for the corrosion of cold rolled steel in 0.5 M sulfuric acid. *J. Mater. Sci.* 41, 3063–3069.
- Xueyuan, Z., Fengping, W., Yufang, H., Yuanlong, D., 2001. Study of the inhibition mechanism of imidazoline amide on CO₂ corrosion of Armco iron. *Corros. Sci.* 43, 1417–1431.